KU LEUVEN

Faculty of Engineering Science
Department of Mechanical Engineering
Control theory [H04X3a]

Report Assignment 3: State Feedback and State Estimation

Academic year 2021 – 2022

Matthias Derez, Toon Servaes

Contents

List of Figures

List of Tables

1 Design of the State Feedback Controller

In this Section, a state feedback controller is designed in order to control the position of the cart while driving on a straight line. This position control loop is then added on top of the velocity controllers designed in Assignment 2.

1.1 Input & Output

Figure 1 visualizes the discrete time LTI system that is examined in this assignment. The input and output are given by:

$$\begin{aligned} \text{input } u(t) &= v(t) = R\omega(t) = \dot{x}(t) \\ \text{output } y(t) &= -x(t) \end{aligned} \tag{1}$$

where $v(t)$ is the velocity of the cart, R the radius of the wheels and ω the rotational velocity of the wheels. The minus sign in the output equation is due to choice of the coordinate system, so that $-x$ represents a positive value.

1.2 State Space Model

There is only one state, the position x, so the matrices in the state equation (and measurement equation) are scalars.

Continuous state space model:

$$\begin{cases} \dot{x}(t) = v(t) = u(t) & \text{state equation} \\ y(t) = -x(t) & \text{measurement equation} \end{cases} \tag{2}$$

Discretization using Forward-Euler scheme:

$$\dot{x}[k] = \frac{x[k+1] - x[k]}{T_s} + O(T_s^2) \tag{3}$$

leads to:

$$\begin{cases} \dot{x}[t+1] = x[k] + T_s u[k] & \text{state equation} \\ y[t] = -x[t] & \text{measurement equation} \end{cases} \tag{4}$$

with T_s the sampling time of 0.01 s. From the general discretized state space form, one can deduce that $A = 1$, $B = T_s$, $C = -1$ and $D = 0$.

1.3 Close Loop Transfer Function

Assuming full state feedback, the closed loop transfer function is:

$$\begin{aligned} H(z) = \frac{Y(z)}{R(z)} &= (C - DK)(z - A + BK)^{-1}B + D \\ &= -(z - 1 + T_s K)^{-1} T_s \\ &= \frac{-T_s}{z - 1 + T_s K} \end{aligned} \tag{5}$$

with K the state feedback gain. Subsequently, the closed loop system has one pole, which is located at

$$p_d = 1 - T_s K \tag{6}$$

This equation indicates that the pole moves to the left for increasing K, or inversely, move to the right for decreasing K, as seen in Figure 2. In the discrete time domain, the system is stable if the poles are within the unit circle. For this particular system, this means $0 < K < 200$ Hz.

However, discrete time poles on the negative side of the real axis have no physical meaning, as these are purely digital effects that have no use in practice. Thus, the state feedback gain is restricted as follows: $0 < K \leq 100$ Hz.

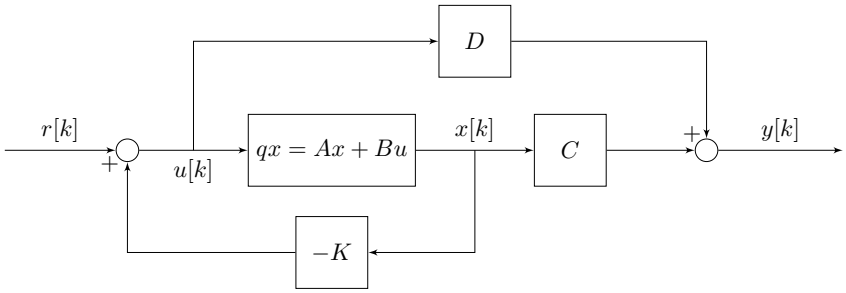

Figure 1: Flow diagram of the closed loop system. [1]

Furthermore, a pole that is close to the unit circle, e.g. for $K = 10$, leads to a slower responding system. Equivalently, a pole that is closer to the origin leads to a faster response. These conclusions are demonstrated by Figure 4.

There are two limit cases. On the one hand, when the pole is located on the unit circle itself, the system is marginally stable. On the other hand, a pole which lies at the origin corresponds to an infinitely fast system, i.e. resulting in a pure time delay of one sample period. This would however mean that the control signal would be infinitely large, thus saturating the actuators. This limits the state feedback gain to $0 < K < 100$ Hz. So there is a trade-off between response time and cost in terms of required actuation signal. Both of these limit cases are depicted in Figure 4.

The previously made conclusions can also be verified by transforming the poles to continuous time and plotting them in the imaginary plane. For continuous time poles, the further the pole lies from the imaginary axis (in the left hand plane), the faster the response. This is confirmed by Figure 3. Note that the continuous time poles are not complex conjugates, which seems incorrect. This is however due to the previously discussed digital effects that have no physical meaning.

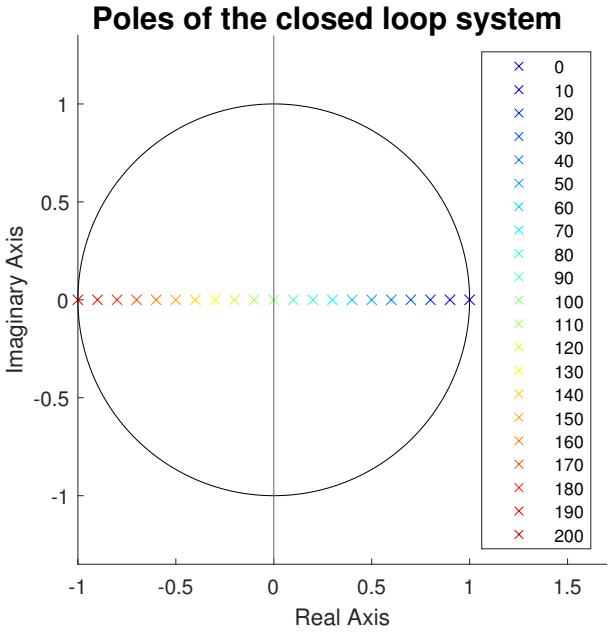

Figure 2: Discrete time pole locations of the closed-loop system for varying values of the state feedback gain.

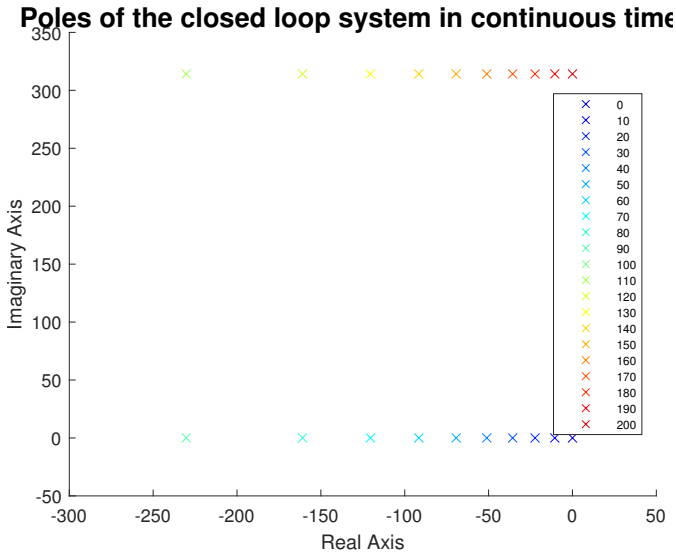

Figure 3: Continuous time pole locations of the closed-loop system for varying values of the state feedback gain.

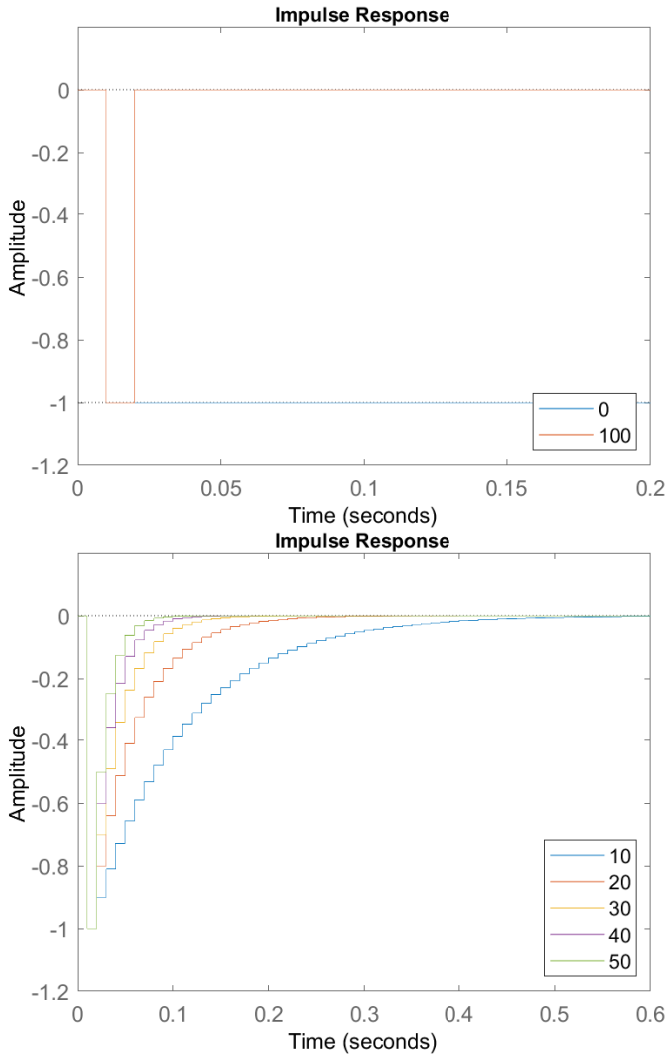

Figure 4: Impulse response of the closed-loop system for varying values of the state feedback gain K.

2 Kalman Filter

As previously elaborated, the measurement equation is equal to

$$y[t] = -x[t] \tag{7}$$

so the C and D matrices of the state-space model are scalar values, respectively -1 and 0. In this Section, these values are used to validate the principles of the Kalman filter on this system. To this extent, some mathematical derivations are done.

2.1 Kalman Gain

Firstly, an expression for the time-varying Kalmain gain L_{k+1} is derived as a function of the state estimate covariance $\hat{P}_{k|k}$, the process noise covariance Q and measurement noise covariance R. This starts from the following equations in Chapter 10 of *Control Theory - Handouts* [2]:

$$\mathbf{L}_{k+1} = \hat{\mathbf{P}}_{k+1|k}\mathbf{C}^T S_{k+1}^{-1} \tag{8}$$

$$S_{k+1} = \mathbf{C}\hat{\mathbf{P}}_{k+1|k}\mathbf{C}^T + R_{k+1} \tag{9}$$

$$\hat{\mathbf{P}}_{k+1|k} = \mathbf{A}\hat{\mathbf{P}}_{k|k}\mathbf{A}^T + \mathbf{Q}_k \tag{10}$$

All matrices and vectors are scalar values in this specific system, so from now on, the boldface notation is left out. Inserting Equations (8) and (9) in Equation (10) and using $A = 1$ and $C = -1$ yields:

$$\begin{aligned} L_{k+1} &= -\left(\hat{P}_{k|k} + Q_k\right)\left(\hat{P}_{k+1|k} + R_{k+1}\right)^{-1} \\ &= -\frac{\hat{P}_{k|k} + Q_k}{\hat{P}_{k+1|k} + R_{k+1}} \\ &= -\frac{\hat{P}_{k|k} + Q_k}{\hat{P}_{k|k} + Q_k + R_{k+1}} \end{aligned} \tag{11}$$

where Equation (10) was used again in the last step.

Taking the limit for $Q_k \to \infty$ results in $L_{k+1} = -1$, which in turn leads to $\hat{x}_{k+1|k+1} = -y_{k+1}$. This is literally the measurement equation of the state-space model (7). One can explain this as follows: the larger Q, the greater the variation of the process noise, the less confidence in the model. Or equivalently, the more confidence in the measurement. In the extreme case, i.e. $Q_k \to \infty$, one has so little confidence in the model that the state equation is entirely neglected.

Next, taking the limit for $R_{k+1} \to \infty$ prompts $L_{k+1} = 0$, which results in $\hat{x}_{k+1|k+1} = \hat{x}_{k+1|k}$. The a priori state estimate is equal to the a posteriori state estimate, meaning that the correction step in the Kalman filter process is neglected. This is yet again easily explainable: the larger R, the greater the variation of the measurement noise, the less confidence in the measurement. Or equivalently, the more confidence in the model. The extreme case $R_{k+1} \to \infty$ has so little confidence in the measurement that the innovation residual is completely not taken into account, thus eliminating the correction step.

2.2 Next State Estimate Covariance

Secondly, an expression for the next state estimate covariance $\hat{P}_{k+1|k+1}$ is derived as a function of the previous state estimate covariance $\hat{P}_{k|k}$, the process noise covariance Q and measurement noise covariance R. Again, starting from an equation given in the handouts:

$$\hat{P}_{k+1|k+1} = (1 - L_{k+1}C)\hat{P}_{k+1|k} = (1 + L_{k+1})\hat{P}_{k+1|k} \tag{12}$$

Using Equations (10) and (11) yields:

$$\begin{aligned}\hat{P}_{k+1|k+1} &= \left(1 - \frac{\hat{P}_{k|k} + Q_k}{\hat{P}_{k|k} + Q_k + R_{k+1}}\right)\hat{P}_{k+1|k} \\ &= \frac{R_{k+1}}{\hat{P}_{k|k} + Q_k + R_{k+1}}\left(\hat{P}_{k|k} + Q_k\right)\end{aligned} \tag{13}$$

Taking the limit for $Q_k \to \infty$ results in $\hat{P}_{k+1|k+1} = R_{k+1}$. Again, $Q_k \to \infty$ indicates that there is zero confidence in the model, so only the measurements get used to adapt the state estimate. This way, the reliability of the estimator is purely based on the reliability of the measurement. In other words, the uncertainty on the state estimate evolves according to the measurement noise covariance. Whereas this uncertainty evolves depending on both the model and the measurements in normal operation of the filter.

Further, the limit for $R_{k+1} \to \infty$ prompts $\hat{P}_{k+1|k+1} = \hat{P}_{k|k} + Q_k = \hat{P}_{k+1|k}$. Once more, $R_{k+1} \to \infty$ indicates zero confidence in the measurements. The a priori covariance matrix of the estimation error is equal to the a posteriori covariance matrix, so the correction step in neglected. In other words, the reliability of the estimator is purely based on the reliability of the model. In normal operation of the filter, $\hat{P}_{k+1|k+1} \preceq \hat{P}_{k+1|k}$, meaning that the uncertainty of the state estimate decreases, whereas in this limit case, the uncertainty does not decrease after the correction step, but it stays the same.

2.3 Steady State Covariance

Now, an expression for the steady state covariance $\hat{P}_\infty$ and the related Kalman gain L_∞ is obtained as a function of Q and R. For this, $\hat{P}_{k|k} = \hat{P}_{k+1|k+1} = \hat{P}_\infty$, $R_{k+1} = R_\infty$ and $Q_k = Q_\infty$ are inserted in Equation (13):

$$\hat{P}_\infty = \frac{R_\infty}{\hat{P}_\infty + Q_\infty + R_\infty}\left(\hat{P}_\infty + Q_\infty\right) \tag{14}$$

Solving for $\hat{P}_\infty$ gives:

$$\hat{P}_\infty = \frac{-Q_\infty \pm \sqrt{Q_\infty^2 + 4R_\infty Q_\infty}}{2} \tag{15}$$

As all covariances must be positive numbers, the only solution for the steady state covariance is:

$$\hat{P}_\infty = \frac{-Q_\infty + \sqrt{Q_\infty^2 + 4R_\infty Q_\infty}}{2} \tag{16}$$

Analogously, these steady state covariances are inserted in Equation (11) in order to find the related steady state Kalman gain:

$$L_\infty = -\frac{\hat{P}_\infty + Q_\infty}{\hat{P}_\infty + Q_\infty + R_\infty} \tag{17}$$

With $\hat{P}_\infty$ equal to Equation (16), L_∞ is likewise expressed as a function of the steady state process noise covariance Q_∞ and the steady state measurement noise covariance R_∞.

In steady state, i.e. $k \to \infty$, the optimal Kalman gain L_{k+1} should converge to the estimator gain L of a Linear Quadratic Estimator. This is verified by computing L_∞ for various numerical values of Q_∞ and R_∞ using the derived equation. It is then compared to the result using the `dlqr(A',A'*C',Q,R)'` command in `Matlab`. E.g. $Q = 0.01$ and $R = 0.01$ leads to $L = -0.9161$ in both cases. One can conclude that the derived formula is correct.

2.4 Closed Loop Pole of the LQE

Lastly, an expression for the closed-loop pole of the Linear Quadratic Estimator is derived as a function of $\frac{Q}{R}$. Generally, the estimator state equation is given by

$$\hat{x}_{k+1} = (A - LC)\hat{x}_k + (B - LD)u_k + Ly_k \tag{18}$$

In this way, the closed loop poles of the estimator are calculated as the eigenvalues of the matrix (A-LC):

$$\det(p_d I - (A - L_\infty C)) = 0 \tag{19}$$

Using the previously calculated scalar values of A and C and using Equations (16) and (17) yields:

$$\begin{aligned} p_d &= 1 + L_\infty \\ &= 1 - \frac{\hat{P}_\infty + Q_\infty}{\hat{P}_\infty + Q_\infty + R_\infty} \\ &= \frac{R_\infty}{\hat{P}_\infty + Q_\infty + R_\infty} \\ &= \frac{2R_\infty}{-Q_\infty + \sqrt{Q_\infty^2 + 4R_\infty Q_\infty} + 2Q_\infty + 2R_\infty} \\ &= \frac{2}{\frac{Q_\infty}{R_\infty} + 2 + \sqrt{\left(\frac{Q_\infty}{R_\infty}\right)^2 + \frac{4Q_\infty}{R_\infty}}} \end{aligned} \tag{20}$$

From this equation, one can deduce that the pole goes to zero with increasing $\frac{Q}{R}$. Inversely, for decreasing ratio ($\frac{Q}{R} \to 0$), the value of the pole shifts towards 1. These conclusions are verified by Figure 5. For $\frac{Q}{R} = 0$, the pole lies on the unit circle, which implies that the system is marginally stable for this ratio. This is the only $\frac{Q}{R}$ - value that leads to instability, because, as depicted by the figure, the poles move towards the centre of the unit circle for increasing values of the ratio. In turn, it means that the systems responds faster and faster. This can easily be explained: the larger $\frac{Q}{R}$, the more confidence in the measurement. Subsequently, the system is more sensitive to measurement noise, which complies with a faster, more nervous tracking of the system.

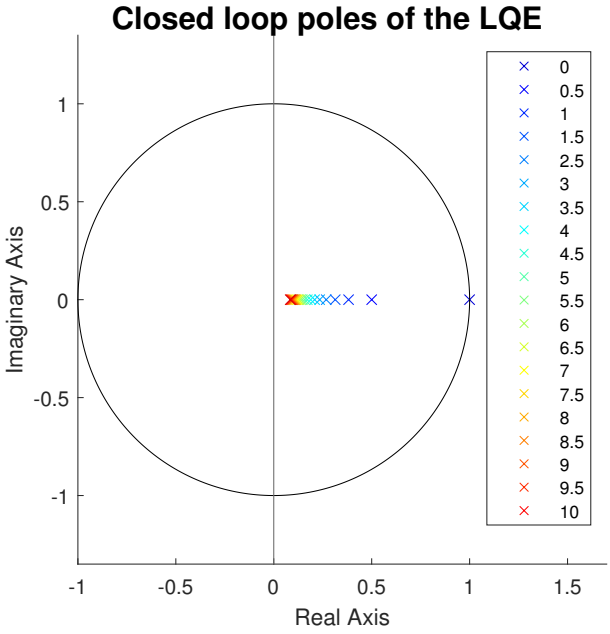

Figure 5: Closed loop poles of the Linear Quadratic Estimator for varying values of the ratio between Q and R, respecitvely the covariance of the process noise and the covariance of the measurement noise.

3 Implementation of a State Estimator and a State Feedback Controller

Yayeet

References

[1] Siang Lim. Control block diagram with tikz. `https://www.overleaf.com/latex/examples/control-block-diagram-with-tikz/jfdcfxhgjmtz`, 2017. Last accessed December 8th 2021.

[2] Swevers J. Pipeleers G. *Control Theory - Handouts*. Cursusdienst VTK, 2021.